# Super- and sub-Lorentzian effects in the Ar-broadened line wings of HCl gas

Ha Tran, Gang Li, Volker Ebert, Jean-Michel Hartmann

# Super- and sub-Lorentzian effects in the Ar-broadened line wings of HCl gas

Ha Tran, Gang Li, Volker Ebert, and Jean-Michel Hartmann

Citation: The Journal of Chemical Physics **146**, 194305 (2017); doi: 10.1063/1.4983397
View online: http://dx.doi.org/10.1063/1.4983397
View Table of Contents: http://aip.scitation.org/toc/jcp/146/19
Published by the American Institute of Physics



# Super- and sub-Lorentzian effects in the Ar-broadened line wings of HCl gas

Ha Tran,[1,a)] Gang Li,[2] Volker Ebert,[2,3,4] and Jean-Michel Hartmann[5]
[1]*Laboratoire de Météorologie Dynamique, IPSL, CNRS, Sorbonne Universités, UPMC University Paris 06, 75252 Paris, France*
[2]*Physikalisch-Technische Bundesanstalt, Bundesallee 100, 38116 Braunschweig, Germany*
[3]*Physikalisch Chemisches Institut, U Heidelberg, INF 253, 69116 Heidelberg, Germany*
[4]*Center of Smart Interfaces, TU Darmstadt, Petersenstraße 32, Darmstadt 64287, Germany*
[5]*Laboratoire de Météorologie Dynamque, IPSL, CNRS, Ecole Polytechnique, Université Paris-Saclay, 91128 Palaiseau, France*

(Received 16 March 2017; accepted 1 May 2017; published online 18 May 2017)

Using previously recorded spectra of HCl diluted in Ar gas at room temperature for several pressure conditions, we show that the absorptions in between successive P and R transitions are significantly different from those predicted using purely Lorentzian line shapes. Direct theoretical predictions of the spectra are also made using requantized classical molecular dynamics simulations and an input HCl–Ar interaction potential. They provide the time evolution of the dipole auto-correlation function (DAF) whose Fourier-Laplace transform yields the absorption spectrum. These calculations very well reproduce the observed super-Lorentzian behavior in the troughs between the intense lines in the central part of the band and the tendency of absorption to become sub-Lorentzian in the band wings between high $J$ lines. The analysis shows that the former behavior is essentially due to incomplete collisions which govern the DAF at very short times. In addition, the increasing influence of line-mixing when going away from the band center explains the tendency of absorption to become more and more sub-Lorentzian in the wings. *Published by AIP Publishing.* [http://dx.doi.org/10.1063/1.4983397]

## I. INTRODUCTION

In a pioneering experimental study,[1] Benedict *et al.* demonstrated in 1956 that the absorptions in the troughs between transitions of the 1-0 band of pure HCl gas exceed those predicted using purely Lorentzian line shapes. A similar behavior was observed[2] sixteen years later for HCl diluted in $CO_2$, and an empirical line shape was proposed for this system. It was only fifteen years later that a theoretical explanation was proposed in a study[3] including new measurements. Using a quasistatic approach[4,5] and neglecting line-mixing effects,[5] Houdeau *et al.* showed[3] that the Lorentz widths of $CO_2$-broadened HCl transitions increase with the distance to line center. This behavior was convincingly attributed to the finite duration of collisions and associated (very) short time behavior of the dipole autocorrelation function. However, this study and the model proposed have several limitations. The first is that a quasistatic approach was used, which is only adapted for the (relatively) far wings.[4,5] The second is that line-mixing effects were disregarded. Such an approximation, likely valid in the central region of the band, nevertheless breaks down in the band wings and the regions around P($J$) and R($J$) lines for large $J$ values (as discussed in Ref. 3). Finally, comparisons with measurements were made for the trough between the P(3) and P(4) lines only. The problem has been on standby since 1985 with, to the best of our knowledge, neither new measurement nor theoretical study.

In the present study, we revisit this issue experimentally and theoretically for HCl diluted in Ar at room temperature. Using previously recorded spectra in both the fundamental[6] and the first overtone[7] bands, we determined the absorptions in the troughs between successive transitions from the P(9) to the R(8) line. Comparisons with predictions using purely Lorentzian line shapes confirm, for both bands, that the absorption is super-Lorentzian in between the intense lines of the central part of the spectra. They also show, for the first time, that this behavior decreases when going away from the band center and that the absorptions become sub-Lorentzian in the high $J$ line regions. A theoretical approach is also proposed in which the dipole autocorrelation function (whose Fourier-Laplace transform yields the spectrum) is directly calculated using requantized Classical Molecular Dynamics Simulations[8,9] (CMDS) based on an input HCl–Ar intermolecular potential. Such calculations, free of any adjusted parameter, intrinsically take line-mixing effects and the finite duration of collision into account. They thus predict the entire spectrum, including the regions around line centers as well as the troughs between lines and the band wing. They lead, as shown thereafter, to a very satisfactory agreement with the observed non-Lorentzian effects.

## II. EXPERIMENTAL DATA USED

The spectra of HCl diluted in Ar used here, as well as the setups and experimental conditions used to record them, are described in Refs. 6 and 7 for the 1-0 and 2-0 bands, respectively. Briefly, in Ref. 6, a Bruker IFS66V Fourier transform spectrometer was used, equipped with a Globar source

a)Author to whom correspondence should be addressed. Electronic mail: htran@lmd.jussieu.fr

and a KBr beam splitter, together with a 2.19 m long high pressure cell and an InSb detector. Argon pressures ranging from about 10 to 50 bars were used with various (very) small relative amounts of HCl. A spectral resolution of 0.12 $cm^{-1}$ was used. The 2-0 band was measured at a resolution of 0.075 $cm^{-1}$ using a Bruker Vertex 80 FTIR spectrometer equipped with a tungsten lamp, a KBr beam splitter, and an InGaAs detector with the argon partial pressure ranging from approximately 1 to 10 bars. The identical setup was also used in Ref. 10. In these studies, essentially devoted to the determination of the spectroscopic line parameters, the measured absorptions were fit near line centers using Voigt (or Lorentz) profiles, yielding the positions (including the pressure shift), Lorentz width, and integrated intensities of the transitions. Based on these retrieved spectroscopic parameters, we have computed spectra under the exact experimental conditions of Refs. 6 and 7 using purely Voigt (or Lorentz) line shapes. This was made not only near the line centers but also over the entire band, thus including the wings and the troughs between transitions. A comparison between a spectrum calculated this way and the associated measured one is plotted in Fig. 1. This example reveals a super-Lorentzian behavior in between the lines within the central region of the band, which is similar to that observed[2] for HCl–$CO_2$ mixtures. It also shows that the absorption becomes sub-Lorentzian when going away from the center, toward high $J$ lines and the band wings. Note that the measured and calculated spectra agree well at the line centers, their ratio being there very close to unity.

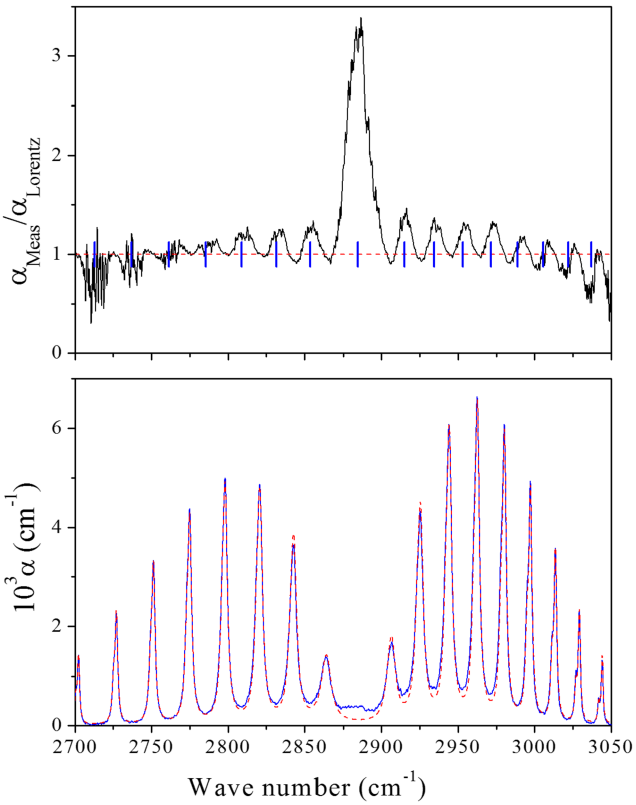


FIG. 1. The lower panel displays the measured absorption coefficient (blue line) and associated purely Lorentzian calculation (red dashed line) in the 1-0 band for 2.5 mbar of HCl diluted in 50.1 bar of Ar at room temperature. Their ratio is plotted in the upper panel where the horizontal red dashed line indicates the unity value and the vertical blue bars show the spectral positions of minimum absorption.

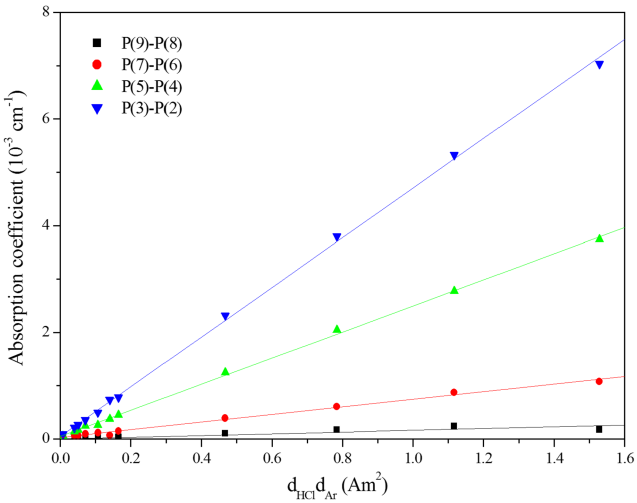


FIG. 2. Measured absorption coefficients vs the product of the densities in amagat unit (Am, 1 Am = $2.687 \times 10^{25}$ mol/m$^3$) of HCl and Ar in some troughs between P($J$) lines of the 1-0 band (symbols) and associated linear fits (lines).

In order to average the various experimental results and have an overall view of non-Lorentzian effects, we retained the spectral points of minimum absorption in the troughs between successive lines. Local fits of measured spectra were made using a second order polynomial for a more precise determination of the absorption minimum. We then looked at the results obtained this way versus the product of the densities of HCl and Ar. As shown in Fig. 2, the behavior is nicely linear as expected in the line wings for a highly diluted mixture. Linear fits were then applied to the values retrieved from both measured and Lorentzian-calculated results, providing the density-normalized values ($\alpha^0_{Meas}$ and $\alpha^0_{Lorentz}$) of the absorptions in the troughs and the associated ratios $\alpha^0_{Meas}/\alpha^0_{Lorentz}$. The latter is the quantity retained for the quantification of non-Lorentzian effects and comparisons with calculations presented in Sec. IV.

## III. CLASSICAL MOLECULAR DYNAMICS SIMULATIONS

Classical Molecular Dynamics Simulations (CMDS)[11] have been performed for highly diluted HCl–Ar mixtures at room temperature and at total densities of 1, 3, and 10 amagat. Each molecule M is characterized by its center-of-mass position $\vec{q}_M(t)$ and velocity $\dot{\vec{q}}_M(t)$, by a unit vector $\vec{u}_M(t)$ along the molecular axis and by its rotational angular velocity vector $\vec{\omega}_M(t)$ [or, alternatively $\dot{\vec{u}}_M(t)$]. The time evolution of the system is governed by interactions among all molecules. Based on an input intermolecular potential and on the initial conditions [i.e., $\vec{q}_M(0)$, $\dot{\vec{q}}_M(t)$, $\vec{u}_M(0)$, and $\vec{\omega}_M(t)$ see below], the evolution of the above mentioned molecular parameters are computed using classical mechanics, as done previously (e.g., Refs. 8 and 9). Here, a total number of $N_M = 2 \times 10^7$ molecules and atoms, placed in 5000 cubic boxes with periodic boundary conditions, was treated in each of the calculations. The latter were carried out on the IMB Blue Gene/P parallel computer of the

*Institut du Développement et des Ressources en Informatique Scientifique*. The molecules' coordinates, the intermolecular potential used, and the calculation procedure are the same as those described in Ref. 9, where details other than those given below can be found. The initial center-of-mass distances between the molecules are imposed to be larger than 8 Å in order to ensure that unphysical strong intermolecular interactions are absent at $t = 0$. The initial orientations of the translational and angular velocities of all molecules have been randomly chosen (as the orientations of the molecules axes) while their modulus obeys the Maxwell-Boltzmann distribution. After several tests, temporization times[11] of about 100, 30, and 10 ps were retained for calculations at 1, 3, and 10 amagat, and a time step of $dt = 1$ fs was used. At each time $t$, the force and torque applied to each molecule/atom by its neighbors are computed. The center-of-mass position $\vec{q}_M(0)$ and velocity $\dot{\vec{q}}_M(t)$, as well as the molecule orientation $\vec{u}_M(t)$ and its angular velocity $\vec{\omega}_M(t)$ are then incremented from $t$ to $t + dt$.

The normalized auto-correlation function $\phi^{rCMDS}(t)$ of the molecular dipole $\vec{\mu}(t)$ is computed since the latter is carried by the molecular axis $\vec{u}(t)$, from

$$\phi^{rCMDS}(t) = \frac{1}{N_M} \sum_{M=1,N_M} \vec{u}_M(t) \cdot \vec{u}_M(0) = \frac{1}{N_M} \sum_{M=1,N_M} \cos\left[\theta_M(t)\right]. \tag{1}$$

Note that the time zero retained for the calculation of $\phi^{rCMDS}(t)$ is not the starting one of the CMDS, but the temporization time defined above. The requantization procedure proposed in Ref. 9 was applied, i.e., starting from $\theta_M(0) = 0$ the angle $\theta_M(t)$ is incremented at each time step using

$$\theta_M(t+dt) = \left[\theta_M(t) + \mathrm{sign}_M(t)\,\omega_M^{RQ}(t)\right] \times \cos\left[\vec{u}_M(t), \vec{u}_M(0) \times \vec{u}_M(t+dt)\right], \tag{2}$$

where $\omega_M^{RQ}(t)$ is the requantized value of the classical rotational angular speed $\omega_M(t) = ||\vec{\omega}_M(t)||$ and $sign_M(t) = \pm 1$ depending on the rotation direction. These quantities are determined as follows. First, $\mathrm{sign}_M(t)$ is set to 1 if the component of $\vec{\omega}_M(t)$ along the laboratory frame x axis is positive, and to −1 otherwise. Then we determine the integer $J_M(t)$ such that the rotational energy $\hbar^2 J_M(t)[J_M(t)+1]/(2I)$ is as close as possible to $I||\vec{\omega}_M(t)||^2/2$, where $I$ is the HCl moment of inertia. Now that we know the initial quantum number ($J_i^M = J_M(t)$), we determine the final quantum number $J_f^M$ of the $J_i^M \rightarrow J_f^M$ line to which molecule M contributes by setting $J_f^M = J_i^M + \mathrm{sign}_M(t)$. Then $\omega_M^{RQ}(t)$ in Eq. (2) is simply set to the true spectral position, taken from the HITRAN (HIgh-resolution TRANsmission molecular absorption database)[12] of the HCl line of initial and final states $J_i^M$, $J_f^M$, respectively (alternatively, we may characterize it by $m_M$ with $m = -J_i^M$ for a P(J) line and $m = J_i^M + 1$ for an R(J) line). Note that this does not affect the values of $\vec{u}_M(t)$ and $\vec{\omega}_M(t)$ which keep following their evolutions governed by classical mechanics. Finally, the area normalized absorption coefficient at angular frequency ω is then directly obtained from the Fourier-Laplace transform of $\phi^{rCMDS}(t)$,[5]

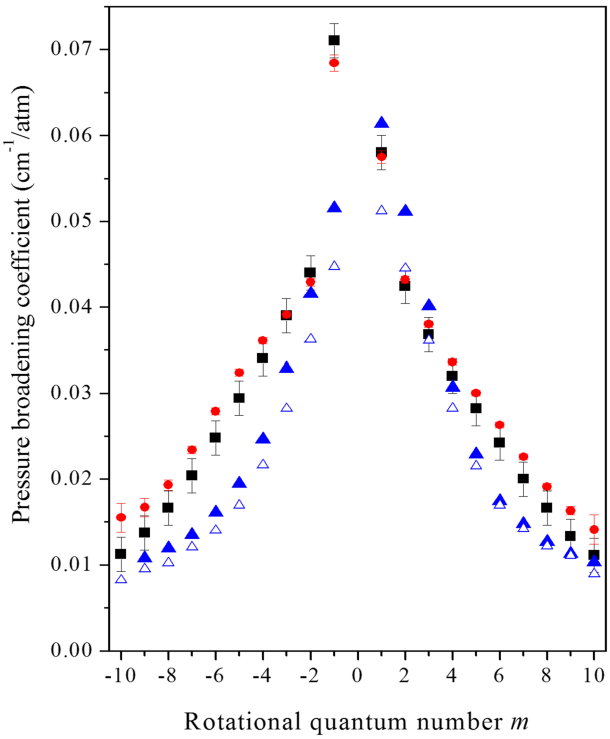


FIG. 3. Ar pressure-broadening coefficients of HCl lines deduced from rCMDS-calculated spectra (blue full triangles), from the temporal evolution of the population $\rho_m(t)$ (blue open triangles) (see Sec. IV), and from measured spectra in the 1-0[6] (black squares) and the 2-0[7] (red circles) bands.

i.e.,

$$\alpha(\omega) = \mathrm{Re}\left[\frac{1}{\pi}\int_0^{+\infty} \phi^{rCMDS}(t) e^{-i\omega t} dt\right]. \tag{3}$$

The rCMDS (requantized classical molecular dynamics simulations) calculated spectra were analyzed with the procedure applied to the measured ones (see Sec. II). Specifically, the following three steps were used: (i) We started from a spectrum calculated for a highly diluted HCl–Ar mixture at 1 amagat and fit it using Lorentz profiles (since the Doppler term was omitted in the rCMDS). This provided the positions, integrated intensities, and Lorentz widths of the transitions. Note that the broadening coefficients obtained, shown by the blue full triangles in Fig. 3, are in satisfactory agreement with measured values, as previously shown.[9] (ii) In a second step, these line parameters were used to simulate, using Lorentz line shapes, a spectrum at 10 amagat. (iii) The values of the absorption at the minima between successive lines were then retrieved from this spectrum and the one directly calculated using rCMDS for the same density. The non-Lorentzian behavior in the troughs between lines was then quantified by the ratio $\alpha_{rCMDS}/\alpha_{Lorentz}$ of these two spectra.

## IV. RESULTS AND DISCUSSION

The experimental and calculated results (i.e., the ratios $\alpha_{obs}/\alpha_{Lorentz}$ and $\alpha_{rCMDS}/\alpha_{Lorentz}$) obtained in the troughs between lines in the P and R branches of the 1-0 and 2-0 bands of HCl diluted in Ar are displayed in Fig. 4. The agreement between measurements and theory is very satisfactory in all troughs from the P(9) to the R(8) lines, except for that between P(1) and R(0) which is discussed below. The rCMDS

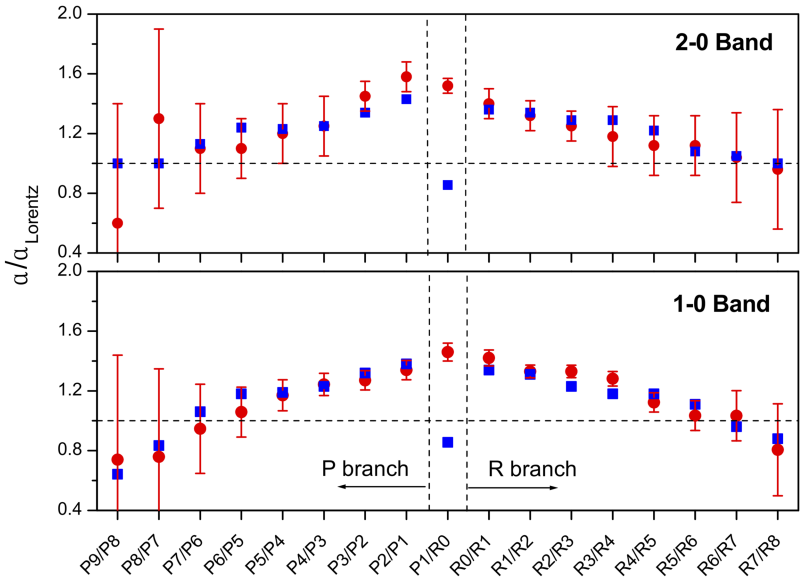


FIG. 4. Comparison between the ratios $\alpha_{rCMDS}/\alpha_{Lorentz}$ obtained from rCMDS-calculated spectra (blue squares) and those determined from experiments, $\alpha_{obs}/\alpha_{Lorentz}$ (red circles with error bars), for HCl diluted in Ar in the 1-0 (lower panel) and 2-0 bands (upper panel) at room temperature. The values (and error bars) between the P(1) and R(0) lines have all been divided by two.

do well reproduce the super-Lorentzian behavior in the central part of the bands, as well as the fact that the absorption becomes sub-Lorentzian when going toward the band edges, in between high $J$ lines. This is, to the best of our knowledge, the first direct and accurate calculation of non-Lorentzian effects over an entire band of HCl. Now considering the troughs at the band centers between the P(1) and R(0) lines, a strongly super-Lorentzian (by a factor of about 3) is observed (Figs. 1 and 4), which is poorly reproduced by the rCMDS. The latter lead to $\alpha_{rCMDS}/\alpha_{Lorentz} = 1.7$, almost a factor of two lower than that determined from measured spectra. For the 1-0 band, a likely explanation for this discrepancy is the fact that, in addition to the cumulated contribution of the wings of all P and R lines on both sides, previous studies[1,2,6] have shown the presence of an absorption structure between the P(1) and R(0) lines. It is discernable through its peak near 2887 $cm^{-1}$ in the bottom plot of Fig. 1, and its amplitude is,[6] for pressures up to 50 atm, comparable to the background due to the line wings that carry it (note that it becomes very significant in the liquid phase[13,14]). As explained in Refs. 6, 13, and 15 and references cited therein, it can be attributed to long-lived Ar–HCl complexes whose contribution is not included in our rCMDS. The resulting calculated spectra thus do not contain absorption due to these complexes and underestimate the absorption near the band center by a factor close to two. Due to experimental noise, it has not been possible to clearly identify an equivalent structure in the first overtone. However, we have no reason to doubt that Ar–HCl complexes also absorb at frequencies close to that of the free HCl 2-0 band, thus also explaining the discrepancies for the central trough of this overtone.

Note that the rCMDS disregard the vibrational dependence of the HCl–Ar potential and its effect on the collisional broadening which results in larger linewidths in the first overtone than in the fundamental (or rotational) band (see Fig. 3 and Ref. 6). In addition, they also do not take the vibrational dephasing into account and thus do not predict any pressure-shifting of the lines. Considering this last approximation, it is likely of very small consequences since the shifts are practically negligible when compared to the spectral separation between successive absorption lines. For the vibrational broadening, neglecting it also has small effects. Indeed, although the calculated widths show non-negligible differences with measured ones (Fig. 3), this has small consequences on the considered ratio of spectra (i.e., $\alpha_{rCMDS}/\alpha_{Lorentz}$). In fact, the consistent errors that are made on both $\alpha_{rCMDS}$ and $\alpha_{Lorentz}$ somehow cancel out when these two absorption coefficients are ratioed out. This small sensitivity of the non-Lorentzian relative effects to the shifts and widths is confirmed by the fact that very similar results are obtained from both experiments and calculations in the 1-0 and 2-0 bands (Fig. 4).

In order to clarify which processes are responsible for the observed non-Lorentzian behaviors, we have determined the relative number $\rho_m(t)$ of molecules that were on a given rotational level $m$ at time $t = 0$ and have remained on the same level until time $t$. Typical results, plotted in Fig. 5, show that two regions are involved. At long time scales, for $t$ larger than a few ps, the populations nicely follow exponential decays with time constants $\tau_m^{\infty}$. On the other hand, for $t$ smaller than a few 0.1 ps, the populations change much more rapidly and do not follow a single exponential decay. It is obvious that, in this short time region, the evolution of $\rho_m(t)$ is essentially governed by the molecules that, at $t = 0$, are experiencing a collision (i.e., are in a significant interaction with an Ar atom). After a fraction of a ps, the associated HCl molecule and Ar atom have moved away from each other and the effect of their interaction vanishes.

In order to go further, recall that, if one neglects both the influence of line-mixing and the contribution of dephasing collisions to the decay of the dipole auto-correlation function (which is then only due to changes of the rotational quantum number $m$), the latter has a simple expression. Indeed, when normalized by the HCl density, it is given, in the collisional regime (no Doppler effect), by

$$\phi(t) = \sum_m S_m \left[\rho_m(t)/\rho_m(0)\right] e^{i\omega_m t}, \tag{4}$$

where $S_m$ is the integrated intensity of the line of rotational quantum number $m$ and $\omega_m$ is its rotational angular frequency. Since the resulting spectrum is obtained from the

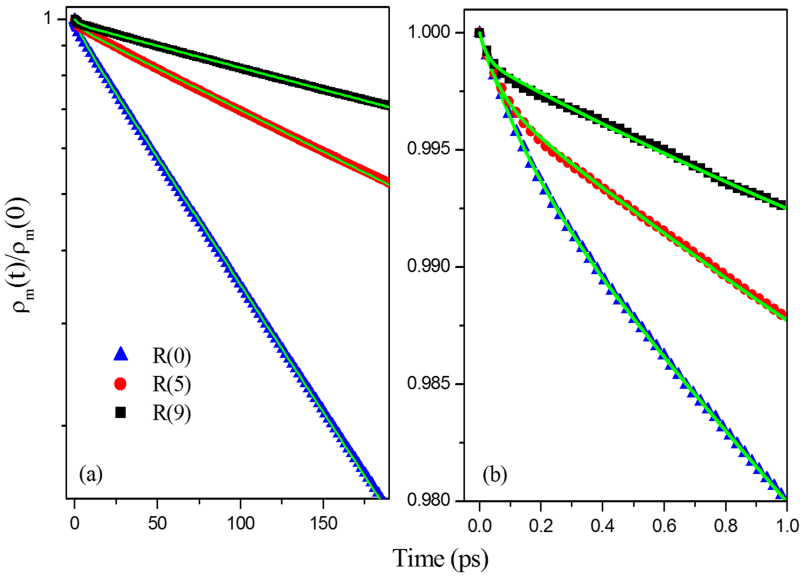


FIG. 5. Normalized populations $\rho_m(t)/\rho_m(0)$ for HCl diluted in Ar at 296 K and 1 amagat, for three rotational quantum numbers $m = 1, 6$, and 10 at different time scales, (a) and (b). The symbols are the rCMDS results, the lines being the fits using Eq. (5). For details see text.

Fourier-Laplace transform of $\phi(t)$, Eq. (4) and Fig. 5 show that it is composed of two components. The first is a sum of Lorentzian line contributions associated with the long time scale exponential decays of $\rho_m(t)$. Indeed, the Fourier-Laplace transform of an exponential leads to a Lorentzian with a half width at half maximum $\Gamma_m^\infty(\text{cm}^{-1}) = (2\pi c\tau_m^\infty)^{-1}$, where $\tau_m^\infty$ is the decay time constant. Note, at this step, that the associated broadening coefficients, denoted in Fig. 3 by the blue open triangles, are in reasonable agreement with measured values. They are slightly smaller than those obtained from the direct rCMDS since dephasing processes are disregarded by the model of Eq. (4). The second component to the spectrum results from the behavior of the populations before typically 1 ps. Since, at these short times the $\rho_m(t)$ vary much more quickly than at longer time scales (see Fig. 5), the Fourier-Laplace transform leads to much broader structures that significantly modify the line wings (and the absorption in the troughs) and thus result in a non-Lorentzian behavior. In order to be more quantitative, we have fit the time evolutions of the various populations using a sum of exponential decays. Since two were not enough for a good adjustment, we used

$$\rho_m(t)/\rho_m(0) \approx a_m^1 e^{-t/\tau_m^1} + a_m^2 e^{-t/\tau_m^2} + a_m^\infty e^{-t/\tau_m^\infty}, \qquad (5)$$

with the imposed condition $a_m^1 + a_m^2 + a_m^\infty = 1$. The quality of these fits is exemplified in Fig. 5. Introducing Eq. (5) into Eqs. (3) and (4) straightforwardly leads to the following expression of the absorption coefficient:

$$\alpha(\sigma) = \frac{1}{\pi}\sum_m S_m d_m^2 \left[\frac{a_m^1\Gamma_m^1}{(\sigma-\sigma_m)^2 + (\Gamma_m^1)^2} + \frac{a_m^2\Gamma_m^2}{(\sigma-\sigma_m)^2 + (\Gamma_m^2)^2} + \frac{a_m^\infty\Gamma_m^\infty}{(\sigma-\sigma_m)^2 + (\Gamma_m^\infty)^2}\right], \qquad (6)$$

with $\sigma \equiv \omega/(2\pi c)$, $\sigma_m \equiv \omega_m/(2\pi c)$ and $\Gamma_m^k \equiv 1/(2\pi c\tau_m^k)$. The spectrum is thus the superposition of three spectra composed of Lorentzian lines with different widths $\Gamma_m^k$ and intensities $S_m a_m^k$ (with k = 1, 2, ∞). It is compared in Fig. 6 with the associated purely Lorentzian one given by

$$\alpha^{Lor}(\sigma) = \frac{1}{\pi}\sum_m S_m \frac{\Gamma_m^\infty}{(\sigma-\sigma_m)^2 + (\Gamma_m^\infty)^2}. \qquad (7)$$

As can be seen, super-Lorentzian absorptions are obtained in the troughs between lines. This confirms that the (very) short time evolution of the dipole auto-correlation function is responsible for this behavior, as concluded in Ref. 3. With respect to the experimental and rCMDS-calculated

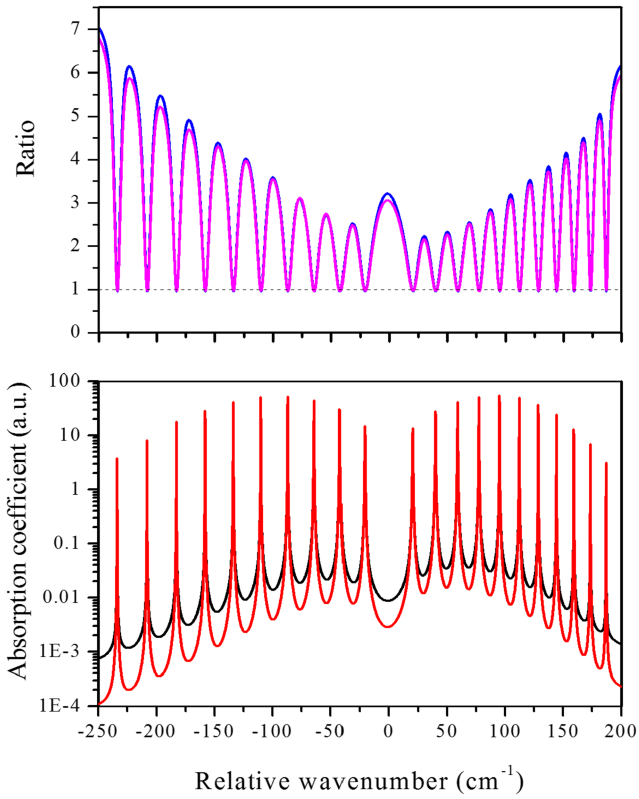


FIG. 6. Bottom: Comparison between spectra of Ar-broadened HCl in the 1-0 band at 3 amagat and 296 K, simulated with the sum of three Lorentzians [Eq. (6)] (black) and with a single one only [Eq. (7)] (red). Top: Ratio between the two simulations at 3 (magenta) and 1 amagat (blue), respectively.

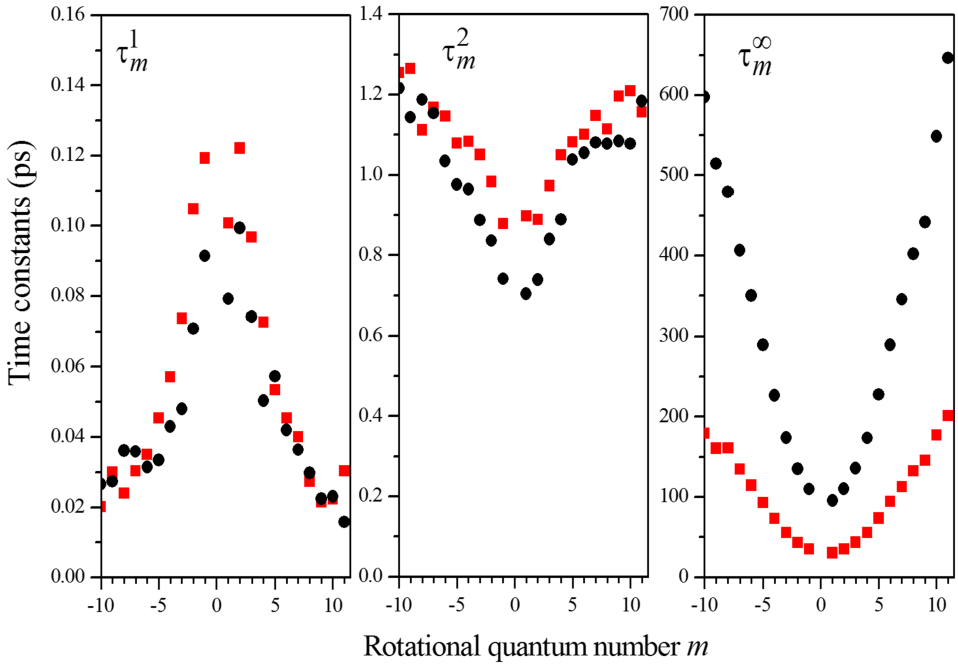


FIG. 7. The relaxation time constants $\tau_m^{1,2,\infty}$ obtained from fits, using Eq. (5) of the normalized populations (e.g., Fig. 5). The red squares and black circles have been obtained from calculations at the densities of 3 and 1 amagat, respectively.

results in Fig. 4, those in Fig. 6 systematically overestimate $\alpha_{rCMDS}/\alpha_{Lorentz}$. Furthermore, the simple model of Eqs. (6) and (7) and Fig. 5 leads to a super-Lorentzian behavior that increases when going toward the band wings, contrary to the results of Figs. 1 and 4. These differences are due to the influence of line mixing, an effect disregarded by this simple model. Indeed, it is well known[5] that line mixing induces transfers of intensity from the band wings and high $J$ line regions toward the band center. In conclusion, the absorption in the troughs between lines results from competitive effects: the short time behavior of the dipole auto-correlation function, which induces super-Lorentzian effects, and line mixing, which acts in the opposite direction. The former has dominant effects near the band center while the latter becomes very efficient in the wings and high $J$ line regions only (for reasons associated with the large rotational constant of HCl, as discussed in Ref. 3).

Let us now discuss the values and density dependence of the parameters $\tau_m^{1,2,\infty}$ and $a_m^{1,2,\infty}$ which are plotted in Figs. 7 and 8, respectively. For the relaxation times, Fig. 7 shows that there are two regimes. The first, governed by the exponentials of time constants $\tau_m^1$ and $\tau_m^2$, is associated with HCl molecules which significantly interact with an Ar atom at time $t = 0$ or shortly after. It is easy to understand that the decays of the population that they induce are independent of the density since they are directly related to the delays needed for an ongoing or a shortly coming collision to be completed. Note that the values in Fig. 7 are consistent with those obtained by considering displacement of a few 0.1 (respectively 5) Å at the

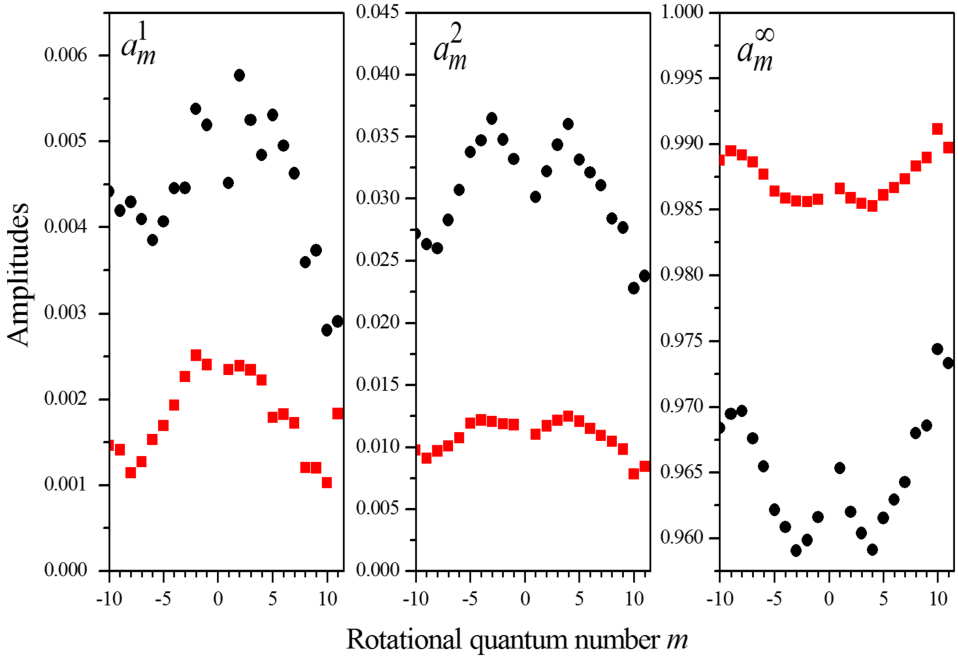


FIG. 8. Amplitudes $a_m^{1,2,\infty}$ obtained from fits, using Eq. (5) of the normalized populations (e.g., Fig. 5). The red squares and black circle have been obtained from calculations at the densities of 1 and 3 amagat, respectively.

mean relative speed (550 m/s). On the other hand, longer time scale decays, governed by $\tau_m^\infty$, involve HCl–Ar pairs which are much further apart at $t = 0$. Since the mean free path is inversely proportional to the gas density, the average delay needed for a collision to occur and thus the associated time constant $\tau_m^\infty$ are also inversely proportional to the density. Note that, if we assume that an efficient collision requires a molecule of HCl to be closer than 5 Å from an Ar atom, the mean free path is, at 1 amagat, of about 500 Å. For a relative speed of 550 m/s, this corresponds to a time interval of 100 ps which is typically the value of $\tau_m^\infty$ for the low J lines. The amplitudes $a_m^{1,2,\infty}$ and their dependences on the density are plotted in Fig. 8. As easily understood, the relative number of molecules, which are experiencing a collision at $t = 0$ or at very shortly times, i.e., the $a_m^1$ and $a_m^2$, are proportional to the density. Indeed, they are governed by the number of Ar atoms within two spheres around an HCl molecule. In order to go further, let us consider the isotropic part of the potential used.[9,14] This could be nicely fitted (not shown here) by a Lennard-Jones potential function versus the distance between the Ar atom and the HCl molecule center of mass with a minimum of −170 K at 3.8 Å. This potential is close to −20 K at 6 Å while its repulsive wall is 300 K at 3.3 Å. Now, for $a_m^1$ which is governed by efficient collisions going on at $t = 0$, the radii of these spheres can be estimated as typically $R_1 \approx 3.3$ Å and $R_2 \approx 3.8$ Å leading to a typical relative number of $N_1 = 4\pi(R_2^3 - R_1^3)d_{\mathrm{Ar}}/3$, where $d_{\mathrm{Ar}}$ is the Ar density. At one amagat, this leads to $N_1 \approx 0.002$, which agrees well with $a_m^1$. For just starting collisions and $a_m^2$, it is reasonable to consider $R_2 \approx 6$ Å and $R_1 \approx 3.8$ Å, leading to $N_1 \approx 0.018$, which is indeed close to the values of $a_m^2$.

## V. CONCLUSION

Using previously recorded spectra in the fundamental and first overtone bands of HCl diluted in Ar gas, we show that the absorption in the troughs between the intense lines in the central part of both bands exceeds that predicted using Lorentzian line shapes. On the other hand, the troughs between lines of high rotational quantum numbers $J$ on the edges of the bands are increasingly sub-Lorentzian as one goes away from the band center. First principle direct calculations of spectra are carried out using requantized molecular dynamics simulations. The latter lead to a very good agreement with measurements and enable to clarify the processes involved. They show that the observed non-Lorentzian absorption results from two competitive mechanisms: (i) the behavior of the dipole autocorrelation at short times (related with collisions that are ongoing or start at t = 0) which induces super-Lorentzian effects; (ii) line-mixing (i.e., transfers of populations among the rotational levels) that reduces the absorption in the band wings and high $J$ line regions and induces sub-Lorentzian effects.

## ACKNOWLEDGMENTS

H. Tran thanks the *Institut du Développement et des Ressources en Informatique Scientifique* (IDRIS) for giving access to the IBM Blue Gene/Q parallel computer. V. Ebert and G. Li acknowledge the strong measurement support by Michael Gisi. Evaluation of the 2-0 band spectra was partially embedded in the EUMETRISPEC project within the European metrology research program (EMRP). The EMRP is jointly funded by the EMRP participating countries within EURAMET and the European Union.

[1] W. S. Benedict, R. Herman, G. E. Moore, and S. Silverman, Can. J. Phys. **34**, 850 (1956).
[2] P. Varanasi, S. K. Sarangi, and G. D. T. Tejwani, J. Quant. Spectrosc. Radiat. Transfer **12**, 857 (1972).
[3] J. P. Houdeau, C. Boulet, and D. Robert, J. Chem. Phys. **82**, 1661 (1985).
[4] C. Boulet and D. Robert, J. Chem. Phys. **77**, 4288 (1982).
[5] J.-M. Hartmann, C. Boulet, and D. Robert, *Collisional Effects on Molecular Spectra: Experiments and Models, Consequences for Applications* (Elsevier, Amsterdam, 2008).
[6] C. Boulet, P.-M. Flaud, and J.-M. Hartmann, J. Chem. Phys. **120**, 11053 (2004).
[7] G. Li, H. Tran, J.-M. Hartmann, M. Gisi, and E. Volker, "First observation of pronounced super-Lorentzian line shape in the 2-0 band spectra of pure HCl and HCl in argon" (unpublished).
[8] J.-M. Hartmann, H. Tran, N. H. Ngo, X. Landsheere, P. Chelin, X. Lu, A. W. Liu, S. M. Hu, L. Gianfrani, G. Casa, A. Castrillo, M. Lepère, Q. Delière, M. Dhyne, and L. Fissiaux, Phys. Rev. A **87**, 013403 (2013).
[9] H. Tran and J. L. Domenech, J. Chem. Phys. **141**, 064313 (2014).
[10] G. Li, A. V. Domanskaya, H. Tran, M. Gisi, and V. Ebert, "Broadening and shift coefficients for the (2←0) overtone band of HCl (1.76 $\mu$m) induced by exhaust gases CO and $CO_2$," J. Quant. Spectrosc. Radiat. Transfer (published online).
[11] M. P. Allen and D. J. Tildesley, *Computer Simulation of Liquid* (Oxford University Press, Oxford, 1986).
[12] L. S. Rothman, I. E. Gordon, Y. Babikov, A. Barbe, D. Chris Benner, P. F. Bernath, M. Birk, L. Bizzocchi, V. Boudon, L. R. Brown, A. Campargue, K. Chance, E. A. Cohen, L. H. Coudert, V. M. Devi, B. J. Drouin, A. Fayt, J. M. Flaud, R. R. Gamache, J. J. Harrison, J. M. Hartmann, C. Hill, J. T. Hodges, D. Jacquemart, A. Jolly, J. Lamouroux, R. J. Le Roy, G. Li, D. A. Long, O. M. Lyulin, C. J. Mackie, S. T. Massie, S. Mikhailenko, H. S. P. Müller, O. V. Naumenko, A. V. Nikitin, J. Orphal, V. Perevalov, A. Perrin, E. R. Polovtseva, C. Richard, M. A. H. Smith, E. Starikova, K. Sung, S. Tashkun, J. Tennyson, G. C. Toon, V. G. Tyuterev, and G. Wagner, J. Quant. Spectrosc. Radiat. Transfer **130**, 4 (2013).
[13] A. Medina, J. M. M. Roco, A. Calvo Hernández, S. Velasco, M. O. Bulanin, W. A. Herrebout, and B. J. van der Veken, J. Chem. Phys. **116**, 5058 (2002).
[14] A. Medina, J. M. M. Roco, A. Calvo Hernández, and S. Velasco, J. Chem. Phys. **121**, 6353 (2004).
[15] A. P. Kouzov, K. G. Tokhadze, and S. S. Utkina, Eur. Phys. J. D **12**, 153 (2000).